HAL
open science

Hepatocyte-specific glucose-6-phosphatase deficiency disturbs platelet aggregation and decreases blood monocytes upon fasting-induced hypoglycemia

Anouk M La Rose, Venetia Bazioti, Joanne A Hoogerland, Arthur F Svendsen, Anouk G Groenen, Martijn van Faassen, Martijn G S Rutten, Niels J Kloosterhuis, Bertien Dethmers- Ausema, J Hendrik Nijland, et al.

To cite this version:

Anouk M La Rose, Venetia Bazioti, Joanne A Hoogerland, Arthur F Svendsen, Anouk G Groenen, et al.. Hepatocyte-specific glucose-6-phosphatase deficiency disturbs platelet aggregation and decreases blood monocytes upon fasting-induced hypoglycemia. Molecular metabolism, 2021, pp.101265. 10.1016/j.molmet.2021.101265 . inserm-03257584

HAL Id: inserm-03257584

https://inserm.hal.science/inserm-03257584v1

Submitted on 11 Jun 2021

HAL is a multi-disciplinary open access archive for the deposit and dissemination of scientific research documents, whether they are published or not. The documents may come from teaching and research institutions in France or abroad, or from public or private research centers.

L'archive ouverte pluridisciplinaire **HAL**, est destinée au dépôt et à la diffusion de documents scientifiques de niveau recherche, publiés ou non, émanant des établissements d'enseignement et de recherche français ou étrangers, des laboratoires publics ou privés.

Hepatocyte-specific glucose-6-phosphatase deficiency disturbs platelet aggregation and decreases blood monocytes upon fasting-induced hypoglycemia

Anouk M. La Rose[1], Venetia Bazioti[1], Joanne A. Hoogerland[1], Arthur F. Svendsen[2], Anouk G. Groenen[1], Martijn van Faassen[3], Martijn G.S. Rutten[1], Niels J. Kloosterhuis[1], Bertien Dethmers-Ausema[2], J. Hendrik Nijland[3], Gilles Mithieux[4], Fabienne Rajas[4], Folkert Kuipers[1,3], Michaël V. Lukens[3], Oliver Soehnlein[5,6], Maaike H. Oosterveer[2], and Marit Westerterp[1,*]

[1] Department of Pediatrics, [2] European Research Institute for the Biology of Ageing, and [3] Department of Laboratory Medicine, University Medical Center Groningen, University of Groningen, Groningen, The Netherlands

[4] Université Claude Bernard Lyon 1, Université de Lyon, INSERM UMR-S1213, Lyon, France

[5] Institute for Experimental Pathology (ExPat), Center for Molecular Biology of Inflammation (ZBME), University of Münster, Münster, Germany

[6] Department of Physiology and Pharmacology (FyFa), Karolinska Institutet, Stockholm, Sweden

***Corresponding author:**

Marit Westerterp PhD

Department of Pediatrics

University Medical Center Groningen

ERIBA Building 3226 room 04.14

Antonius Deusinglaan 1

9713 AV Groningen

The Netherlands

Phone: +31503616615

E-mail: m.westerterp@umcg.nl

List of nonstandard abbreviations

GSD Ia: glycogen storage disease type 1a

G6PC1: glucose-6-phosphatase catalytic subunit

L-*G6pc*$^{-/-}$: hepatocyte-specific *G6pc1* deficiency

G6P: glucose-6-phosphate

UCCS: uncooked cornstarch

NAFLD: non-alcoholic fatty liver disease

ZT: zeitgeber time

WBC: white blood cell

RBC: red blood cell

CCR2: C-C chemokine receptor 2

CXCR4: C-X-C motif chemokine receptor 4

VLA4: very late antigen-4

LSK: Lin^{-}, Sca1^{+}, cKit^{+} cells

CMP: common myeloid progenitors

GMP: granulocyte/monocyte progenitors

MCP-1: monocyte chemoattractant protein-1

M-CSF: macrophage-colony stimulating factor

G-CSF: granulocyte-colony stimulating factor

FFA: free fatty acid

PNMT: phenylethanolamine *N*-methyltransferase

VLDL-TG: very-low-density lipoprotein-triglycerides

LPL: lipoprotein lipase

vWF: von Willebrand factor

PT: prothrombin time

aPTT: activated partial thromboplastin time

SGLT2: sodium glucose co-transporter 2

GLUT: glucose transporter

PAR4: protease-activated receptor 4 peptide

Abstract

Objective: Glycogen storage disease type 1a (GSD Ia) is a rare inherited metabolic disorder caused by mutations in the glucose-6-phosphatase (*G6PC1*) gene. When untreated, GSD Ia leads to severe fasting-induced hypoglycemia. Although current intensive dietary management aims to prevent hypoglycemia, patients still experience hypoglycemic events. Poor glycemic control in GSD Ia is associated with hypertriglyceridemia, hepatocellular adenoma and carcinoma, and also with an increased bleeding tendency of unknown origin.

Methods: To evaluate the effect of glycemic control on leukocyte levels and coagulation in GSD Ia, we employed hepatocyte-specific *G6pc1* deficient (L-*G6pc*$^{-/-}$) mice under fed or fasted conditions, to match good or poor glycemic control in GSD Ia, respectively.

Results: We found that fasting-induced hypoglycemia in L-*G6pc*$^{-/-}$ mice decreased blood leukocytes, specifically pro-inflammatory Ly6C^{hi} monocytes, compared to controls. Refeeding reversed this decrease. The decrease in Ly6C^{hi} monocytes was accompanied by an increase in plasma corticosterone levels and was prevented by the glucocorticoid receptor antagonist mifepristone. Further, fasting-induced hypoglycemia in L-*G6pc*$^{-/-}$ mice prolonged bleeding time in the tail vein bleeding assay, with reversal by refeeding. This could not be explained by changes in coagulation factors V, VII, or VIII, or von Willebrand factor. While the prothrombin and activated partial thromboplastin time, as well as total platelet counts were not affected by fasting-induced hypoglycemia in L-*G6pc*$^{-/-}$ mice, ADP-induced platelet aggregation was disturbed.

Conclusions: These studies reveal a relationship between fasting-induced hypoglycemia, decreased blood monocytes, and disturbed platelet aggregation in L-*G6pc*$^{-/-}$ mice. While disturbed platelet aggregation likely accounts for the bleeding phenotype in GSD Ia, elevated plasma corticosterone decreases levels of pro-inflammatory monocytes. These studies highlight the necessity of maintaining good glycemic control in GSD Ia.

Keywords

Glycogen storage disease type 1a, hypoglycemia, corticosterone, monocytes, platelets

1. Introduction

Glycogen storage disease type 1a (GSD Ia) is an inborn error of carbohydrate metabolism with an incidence of 1 in 100.000 births [1]. GSD Ia is caused by mutations in the gene encoding the catalytic subunit of the glucose-6-phosphatase enzyme (G6PC1) [2–4]. G6PC1 is expressed in the liver, kidney and intestine and catalyzes the hydrolysis of glucose-6-phosphate (G6P) to glucose [1]. Due to the essential role of G6PC1 in endogenous glucose production, GSD Ia patients present with life-threatening fasting hypoglycemia when untreated [1,5]. To prevent hypoglycemia, patients receive dietary therapy consisting of frequent small doses of the slow release carbohydrate source uncooked cornstarch (UCCS) during the day and UCCS or continuous gastric drip feeding during the night [6,7].

Despite intensive dietary treatment, short periods of hypoglycemia still occur in GSD Ia, generally referred to as poor glycemic control [6,7]. GSD Ia patients show hyperlipidemia, which is aggravated by poor glycemic control [5,8–10]. In addition, they develop severe hepatomegaly and non-alcoholic fatty liver disease (NAFLD) as a consequence of excessive glycogen and lipid accumulation [1,11,12], and hepatocellular adenoma, which may progress into carcinoma [6,7,13,14]. Despite prominent hyperlipidemia, GSD Ia patients show a 10% reduction in carotid intima media thickness [15], reflecting decreased atherosclerotic lesions in the carotid arteries.

Under conditions of poor glycemic control, GSD Ia patients show increased bleeding tendency, which complicates surgical procedures [16–18]. This can be prevented by continuous gastric drip feeding to maintain euglycemia over a period of 24 hours prior to surgery [16–18]. Several pathways have been proposed to decrease atherosclerosis and enhance bleeding in GSD Ia [16,18–20]. The exact mechanisms remain elusive, likely due to the relatively small number of GSD Ia patients included in these studies and the high level of clinical heterogeneity [21]. Hypoglycemia due to poor glycemic control could contribute to the low incidence of atherosclerosis in GSD Ia. Hypoglycemia may decrease blood monocytes, as suggested by others [23]. Low monocyte numbers may decrease atherosclerosis, as well as monocyte-platelet aggregates, which induce coagulation [24,25]. Hypoglycemia may also affect platelet aggregation directly [18,26].

We investigated the effects of glycemic control in GSD Ia on leukocyte levels and coagulation and the mechanisms involved. We used a mouse model of GSD Ia with hepatocyte-specific

G6pc1 deficiency (L-*G6pc*$^{-/-}$ mice) that were studied under fed or fasted conditions, to match good or poor glycemic control in GSD Ia, respectively [10].

2. Materials and Methods

2.1 Animals

Female *B6.G6pc1*$^{lox/lox}$ and *B6.G6pc1*$^{lox/lox}$*.SA*^{CreERT2} mice were housed in a light (lights on at 7:00 AM. *i.e.* Zeitgeber Time (ZT) 0, lights off at 7:00 PM, *i.e.* ZT12) and temperature (21°C) - controlled facility. Mice had free access to water and a standard chow diet (67% carbohydrates, consisting of the low glycemic index carbohydrate sources wheat (glycemic index 54), barley (glycemic index 28) and corn gluten, 23% protein and 10% fat; RMH-B, AB diets, Woerden, The Netherlands). At 8-12 weeks of age, mice received intraperitoneal tamoxifen injections (T5648; Sigma-Aldrich, St. Louis, MO, USA) (1mg/day in 95% sunflower oil/5% ethanol) for five consecutive days to generate hepatocyte-specific *G6pc1* deficient mice (L-*G6pc*$^{-/-}$) and littermate floxed controls (control), as described previously [27]. Female littermates were randomly assigned to experimental groups and the number of mice used for each experiment is indicated in the figure legends. No inclusion or exclusion criteria were used. Experiments were performed over a period of 6-16 weeks after tamoxifen injections at ZT1 (fed), ZT7 (6 hour fast during the inactive period or non-fasted), and, in case of fasting, the next morning at ZT1 (refeeding during the inactive and active period). All animal studies were approved by the Institutional Animal Care and Use Committee from the University of Groningen under permit number AVD105002015244 and adhered to guidelines set out in the 2010/63/EU directive.

2.2 Blood glucose levels

Blood glucose levels were measured using an Accu-Chek Performa glucose meter (Roche, Basel, Switzerland) and Accu-Chek Performa testing strips (06454011; Roche, Basel, Switzerland).

2.3 White blood cell and platelet counts

Blood samples were collected by tail bleeding into EDTA-coated tubes. Total white blood cell (WBC) and platelet counts were measured using the Medonic CD620 hematology analyzer (Boule Medical, Spanga, Sweden).

2.4 Flow cytometry

Blood samples were collected by tail bleeding into EDTA-coated tubes and kept on ice. For analysis of blood leukocyte subsets, samples were kept at 4°C during the whole procedure unless stated otherwise. Red blood cells (RBCs) were lysed for 5 minutes (BD Pharm Lyse; BD Bioscience, Franklin Lakes, NJ, USA) and WBCs were centrifuged, washed and resuspended in HBSS (0.1% BSA and 0.5mM EDTA). To assess monocytes, monocyte subsets, neutrophil, B-cell and T-cell populations, cells were stained with a cocktail of antibodies: CD45-APC-Cy7 (557659; BD Biosciences, Franklin Lakes, NJ, USA), CD115-APC (17-1152-82; eBioscience, San Diego, CA, USA), Ly6C/G-PercP-Cy5.5 (561103; BD Biosciences, Franklin Lakes, NJ, USA), TCRβ-PB (109226; Biolegend, San Diego, CA, USA) and CD19-PE (152408; Biolegend, San Diego, CA, USA) for 30 minutes on ice in the dark. Monocytes were identified as $CD45^{hi}CD115^{hi}$, and further separated into $Ly6C^{lo}$ and $Ly6C^{hi}$ subsets based on the marker Ly6C. Neutrophils were identified as $CD45^{hi}CD115^{lo}Ly6G^{hi}$. Lymphocytes were identified as $CD45^{hi}CD115^{lo}Ly6C^{lo}/G^{lo}$ and further separated into B-cells, identified as $CD19^{hi}$, and T-cells, identified as $TCR\beta^{hi}$. For measurements of monocyte and neutrophil surface marker expression, cells were stained with CD45-APC-Cy7 (557659; BD Biosciences, Franklin Lakes, NJ, USA), CD115-APC (17-1152-82; eBioscience, San Diego, CA, USA) or CD115-PE (135506; Biolegend, San Diego, CA, USA) and Ly6C/G-PercP-Cy5.5 (561103; BD Biosciences, Franklin Lakes, NJ, USA). C-C chemokine receptor 2 (CCR2) -PE (FAB5538P; R&D systems, Minneapolis, MN, USA), CD11b-PB (552093; BD Biosciences, Franklin Lakes, NJ, USA), CD62L-APC (17-0621-81; eBioscience, San Diego, CA, USA), C-X-C motif chemokine receptor 4 (CXCR4) -FITC (551967; BD Biosciences, Franklin Lakes, NJ, USA), CXCR2-APC (149604; Biolegend, San Diego, CA, USA) or very late antigen-4 (VLA4) -PE (553157; BD Biosciences, Franklin Lakes, NJ, USA) were added to this panel.

For analysis of bone marrow leukocyte and progenitor cell populations, the femur and tibia were collected, bone marrow (BM) was harvested and mashed on a 40 μm strainer. RBCs were lysed for 2 minutes on ice. WBCs were centrifuged, washed and resuspended in HBSS (0.1% BSA and 0.5mM EDTA). Total WBC counts were measured using the Medonic CD620 hematology analyzer (Boule Medical, Spanga, Sweden). Leukocyte subsets in BM were assessed by flow cytometry using the staining described above for blood WBCs. For analysis of progenitor

populations, cells were stained with a cocktail of antibodies (all from Biolegend, San Diego, CA, USA, unless stated otherwise): Sca1-BV421 (108127), cKit-APC (105812), CD127-PE (135010), CD16/32-PE-Cy7 (101318), CD34-FITC (553733; BD biosciences, Franklin Lakes, NJ, USA), B220-A700 (103231), CD11b-A700 (101222), CD3-A700 (100216), Ly6C/G-A700 (108422) and Ter119-A700 (116220) for 30 minutes on ice in the dark. Hematopoietic stem and progenitor cells were identified as $CD127^-$, lineage $(Lin)^-$, $Sca1^+$, and $cKit^+$ (LSK). Hematopoietic progenitors were identified as Lin^-, $CD127^-$, $Sca\text{-}1^-$, $cKit^+$ cells and further separated into $CD34^{int}$, $CD16/32^{int}$ common myeloid progenitors (CMP) and $CD34^{int}$, $CD16/32^{hi}$ granulocyte/monocyte progenitors (GMP).

For analysis of hepatic monocytes and neutrophils, livers were collected, digested using collagenase (1.5mg/ml in PBS) (C5138; Sigma-Aldrich, St. Louis, MO, USA) for 45 minutes at 37°C and mashed on a 40 µm strainer. Up to 50ml PBS was added and samples were centrifuged at 70 xg with brake settings off for 5 minutes. The upper layer containing the hepatic leukocytes was centrifuged at 400 xg for 10 minutes and RBCs were lysed for 2 minutes on ice. Samples were centrifuged, washed and resuspended in HBSS (0.1% BSA and 0.5mM EDTA). $CD45^+$ cells were isolated from liver homogenates using CD45 coated magnetic beads (130-052-301; Miltenyi Biotec, Bergisch Gladbach, Germany) according to the manufacturer's instructions. Total WBC counts were measured using the Medonic CD620 hematology analyzer (Boule Medical, Spanga, Sweden). To assess hepatic monocytes and neutrophils, $CD45^+$ cells were stained with CD45-APC-Cy7 (557659; BD Biosciences, Franklin Lakes, NJ, USA), CD11b-PB (552093; BD Biosciences, Franklin Lakes, NJ, USA) and Ly6C/G-PercP-Cy5.5 (561103; BD Biosciences, Franklin Lakes, NJ, USA) as described above for blood WBCs. Monocytes were identified as $CD45^{hi}CD11b^{hi}Ly6C^{hi}SSC^{lo}$ and neutrophils as $CD45^{hi}CD11b^{hi}Ly6G^{hi}SSC^{hi}$.

All samples were analyzed on an LSRII (BD Biosciences, Franklin Lakes, NJ, USA), running FACSDiVa software (BD Biosciences, Franklin Lakes, NJ, USA). Data were analyzed using FlowJo software (FlowJo, Ashland, OR, USA). CCR2 expression was analyzed as mean fluorescence intensity (MFI).

2.5 ELISAs

Blood samples were collected. Plasma was separated by centrifugation and Monocyte chemoattractant protein-1 (MCP-1), macrophage-colony stimulating factor (M-CSF) and granulocyte-colony stimulating factor (G-CSF) were measured using ELISA kits (MJE00, MMC00 and MCS00, respectively; R&D systems, Minneapolis, MN, USA) according to the manufacturer's instructions.

2.6 Mifepristone treatment

Six weeks after tamoxifen injections, mice received an intraperitoneal injection with the glucocorticoid receptor antagonist Mifepristone (M8046; Sigma-Aldrich, St. Louis, MO, USA) (25mg/kg in 90% sunflower oil/10% ethanol) or vehicle at the start of the 6 hour fasting period.

2.7 Plasma triglycerides and lipoprotein analysis

Blood samples were collected. Plasma was separated by centrifugation and plasma triglyceride (TG) and free fatty acid (FFA) levels were measured using enzymatic kits (157109910917 and 157819910935, respectively; Diasys Diagnostic Systems, Holzheim, Germany) with Precimat Glycerol or FFA standard FS (10166588; Roche, Mannheim, Germany and 157809910065; Diasys Diagnostic Systems, respectively) for the calibration curve. Lipoprotein TG distribution was measured by fast performance liquid chromatography (FPLC) using a system containing a PU-4180 pump with a linear degasser and UV-4075 UV/VIS detectors (Jasco, Tokyo, Japan). Pooled plasma samples (n=8-12) were injected onto a Superose 6 Increase 10/300 GL column (GE Healthcare, Hoevelaken, The Netherlands) and eluted at a constant flow rate of 0.31 ml/min in PBS (pH 7.4). Triglycerides were measured in line by addition of TG reagent (157109910917; Diasys, Holzheim, Germany) at a constant flow rate of 0.1 ml/min using an additional PU-4080i infusion pump (Jasco, Tokyo, Japan). Data acquisition and analysis were performed using ChromNav software (version 1.0; Jasco, Tokyo, Japan).

2.8 Flow cytometry of platelet-leukocyte aggregates

For analysis of platelet-leukocyte aggregates, blood was collected by retro-orbital bleeding into tubes containing 3.2% sodium citrate (9:1 v/v) (41.1506.002; Sarstedt, Nümbrecht, Germany) and kept at RT. Samples were kept at 4°C for all subsequent steps. RBCs were lysed for 5 minutes (BD Pharm Lyse, BD Bioscience, Franklin Lakes, NJ, USA), samples were centrifuged, washed and resuspended in HBSS (0.1% BSA and 0.5mM EDTA). To assess platelet-monocyte and platelet-neutrophil aggregation, samples were incubated with a cocktail of antibodies: CD45-APC-Cy7 (557659; BD Biosciences, Franklin Lakes, NJ, USA), CD115-PE (135506; Biolegend, San Diego, CA, USA), Ly6C/G-PercP-Cy5.5 (571103; BD Biosciences, Franklin Lakes, NJ, USA), CD41-FITC (133904; Biolegend, San Diego, CA, USA) for 30 minutes on ice in the dark. Platelet-monocyte aggregates were identified as $CD45^{hi}CD115^{hi}CD41^{hi}$, and were further separated into platelet-$Ly6C^{lo}$ monocyte aggregates, defined as $CD45^{hi}CD115^{hi}Ly6C^{lo}CD41^{hi}$ and platelet-$Ly6C^{hi}$ monocyte aggregates, defined as $CD45^{hi}CD115^{hi}Ly6C^{hi}CD41^{hi}$. Platelet-neutrophil aggregates were identified as $CD45^{hi}CD115^{lo}Ly6G^{hi}CD41^{hi}$. All samples were analyzed on an LSRII (BD Biosciences, Franklin Lakes, NJ, USA), running FACSDiVa software (BD Biosciences, Franklin Lakes, NJ, USA). The data were analyzed using FlowJo software (FlowJo, Ashland, OR, USA).

2.9 Plasma corticosterone, epinephrine and norepinephrine

Blood was collected by retro-orbital bleeding into EDTA coated tubes (450532; Greiner Bio-One, Kremsmünster, Austria) and kept on ice. Plasma was separated by centrifugation and 5 mg reduced glutathione (G4251; Sigma-Aldrich, St. Louis, MO, USA) was added per mL of plasma after centrifugation to prevent degradation of epinephrine and norepinephrine. Plasma was snap-frozen and stored at -80°C until further use. Corticosterone, epinephrine and norepinephrine were measured by online solid phase extraction (SPE) in combination with isotope dilution liquid chromatography tandem mass spectrometry (LC-MS/MS). Corticosterone measurement was performed essentially as described by Hawley et al [28], using corticosterone-D4 as stable isotope labeled internal standard on an online SPE manager in combination with a XEVO TQ mass spectrometer (Waters, Milford, MA, USA). Epinephrine and norepinephrine were analyzed as described by Van Faassen et al [29], using epinephrine-D3 and norepinephrine-D6 as stable isotope labeled internal standard on a Symbiosis Pharma online SPE system (Spark Holland,

Emmen, The Netherlands) in combination with Xevo TQ mass spectrometer (Waters, Milford, MA, USA).

2.10 Adrenal gland mass

Twelve weeks after tamoxifen injections, mice were sacrificed by cardiac puncture in the fed or fasted condition. Adrenal glands were collected, cleaned of surrounding fat and weighed.

2.11 Tail vein bleeding assay

The tail vein bleeding assay was performed as described previously [30]. Briefly, mice were anesthetized with isoflurane. A 10 mm segment of the distal tip of the tail was removed using a scalpel. The tail was immediately immersed in a 50 mL tube containing 50 mL phosphate buffered saline (PBS) pre-warmed to 37°C. Time until bleeding ceased was recorded with a maximum bleeding time of 300 seconds. Volume of blood loss during the bleeding assay was quantified by measuring absorbance at 550nm using a spectrophotometer (Genesys 10S UV-Vis; Thermofisher Scientific, Waltham, MA, USA).

2.12 Prothrombin time, activated partial prothrombin time and plasma coagulation factors

Blood was collected by cardiac puncture into tubes containing 3.2% sodium citrate (9:1 v/v) (41.1506.002; Sarstedt, Nümbrecht, Germany). Samples were immediately centrifuged at RT to collect plasma. Plasma was stored at -80°C until further use. Pro-thrombin time (PT) and activated partial thrombin time (aPTT) were assessed on an automated coagulation analyser (CS-2100i) with reagents (PT-Innovin for PT and ActinFS for aPTT) and protocols from the manufacturer (Siemens, Marburg, Germany). Levels of factor V (FV), VII (FVII) and FVIII (FVIII) were determined on an automated coagulation analyser (CS2100i) based on the one-stage clotting assay with factor-deficient plasma (Siemens, Marburg, Germany). Testing was performed according to the protocols from the manufacturer (Siemens). Levels are shown as percentages of standard human plasma (Siemens, Marburg, Germany).

2.13 Von Willebrand Ristocetin cofactor

Blood was collected by cardiac puncture into tubes containing 3.2% sodium citrate (9:1 v/v) (41.1506.002; Sarstedt, Nümbrecht, Germany). Samples were immediately centrifuged at RT to collect plasma. Plasma was stored at -80°C until use. Von Willebrand Ristocetin cofactor (vWF RCF) levels were determined on a CS2100i coagulation analyzer with the Innovance vWF activity kit (Siemens, Marburg, Germany) according to the protocol from the manufacturer with all equipment and reagents from Siemens (Marburg, Germany).

2.14 Platelet aggregation

To assess platelet aggregation, blood was drawn by cardiac puncture and collected into tubes containing 3.2% sodium citrate (9:1 v/v) (41.1506.002; Sarstedt, Nümbrecht, Germany). Samples were kept at RT during the whole procedure. Samples were centrifuged at 110 xg and platelet rich plasma (PRP) was collected. PRP was diluted to a final concentration of $200^{*}10^{6}$ platelets per mL using platelet poor plasma (PPP) from the same mouse. Platelet aggregation in response to 10µM ADP was measured using light transmission aggregometry (Chrono-log Model 700; Chrono-log Corporation, PA, USA) at 37°C, stirring at 1200rpm. Light transmission was recorded for 10 minutes using AggroLink 8 software.

2.15 Statistical analysis

All data are presented as mean ± SEM. The unpaired t-test was used to compare two datasets. To compare ≥ 3 groups, a one-way ANOVA, with Bonferroni post-hoc test was performed. Group size and statistical tests are reported in the figure legends. The criterion for significance was set at $P<0.05$. Statistical analysis was performed using GraphPad Prism 5 (GraphPad Software; San Diego, CA, USA).

3. Results

3.1 Fasting decreases blood leukocytes in L-*G6pc*$^{-/-}$ mice

We first confirmed that, similar to previous studies [27,31], hepatocyte-specific *G6pc1* deficiency induces hypoglycemia after a fasting period of 6 hours. For this purpose, we measured blood glucose levels at Zeitgeber Time (ZT) 1 (fed), ZT7 (6 hour fast during the inactive period or non-fasted), and the next morning at ZT1 (refeeding during the inactive and active period). In line with previous studies [27], L-*G6pc*$^{-/-}$ mice showed hypoglycemia (blood glucose ≤ 4.0mM) after a 6 hour fast, with average blood glucose levels of ~3.6mM (Figure 1A). Refeeding restored blood glucose levels to ~7.9mM (refeeding; ZT1) (Figure 1A). L-*G6pc*$^{-/-}$ mice maintained euglycemia when not fasted (Figure 1B). This is probably due to the chow diet resembling the dietary therapy given to GSD Ia patients. GSD Ia patients are on a dietary therapy of uncooked cornstarch that has a glycemic index of 48 [32], and as a consequence induces slow release of glucose, preventing hypoglycemia in these patients [7]. Chow diet contains 67% carbohydrates with a glycemic index of 54 and 28 (specified in the methods section), which likely explains why L-*G6pc*$^{-/-}$ mice maintain euglycemia when not fasted. We observed the decrease in blood glucose levels in L-*G6pc*$^{-/-}$ mice upon a 6 hour fast at all time points measured throughout the study (Figure S1A, B).

Previous studies have shown that prolonged fasting (20 hours) leads to hypoglycemia, which decreases blood monocyte levels [23]. We thus assessed whether hepatocyte-specific *G6pc1* deficiency affected blood leukocytes in the fasted and non-fasted condition. While control mice showed an increase in total CD45^{+} blood leukocyte levels after fasting, likely due to circadian rhythmicity [33], L-*G6pc*$^{-/-}$ mice did not (Figure 1C). Refeeding restored blood leukocyte levels in L-*G6pc*$^{-/-}$ mice (ZT1; refeeding) (Figure 1C). We observed no differences in blood leukocytes when L-*G6pc*$^{-/-}$ mice were not fasted and remained euglycemic (Figure 1D). Further analysis of leukocyte subsets in fasted animals showed that hepatocyte-specific *G6pc1* deficiency decreased total monocytes by ~50%, mainly reflected by decreases in pro-inflammatory Ly6C^{hi} and to a lesser extent Ly6C^{lo} monocytes (Figure 1E-I, K, M). Refeeding restored monocyte levels (Figure 1I, K, M). Leukocyte levels were not different between the genotypes in the non-fasted condition (Fig 1J, L, N). We then asked which fasting-induced changes could account for the decrease in blood Ly6C^{hi} monocytes in L-*G6pc*$^{-/-}$ mice during fasting. Blood Ly6C^{hi} monocyte levels showed

a strong correlation with blood glucose levels in L-*G6pc*$^{-/-}$ mice, but not in control mice upon a 6 hour fast (Fig S2; Pearson correlation coefficient r=0.65; p=0.009), suggesting a major contribution of hypoglycemia to the decreased blood monocytes upon fasting. Fasting also increases plasma VLDL-TG and VLDL-cholesterol in L-*G6pc*$^{-/-}$ mice [10]. However, elevated VLDL-cholesterol increases Ly6C^{hi} monocytes in mice [34]. We found that fasting did not affect plasma FFAs in L-*G6pc*$^{-/-}$ mice, although plasma FFAs were elevated in the fed and fasted state, compared to controls (Fig S3). Hence it is unlikely that lipids have contributed to the decreased blood Ly6C^{hi} monocytes in fasted L-*G6pc*$^{-/-}$ mice. While our data suggest that hypoglycemia is a key factor in decreasing blood monocytes, we cannot exclude that hormonal changes in fasted L-*G6pc*$^{-/-}$ mice [35] may have contributed to the decrease in monocytes. Administration of glucose by gavage during the fasting period, as done in wild-type mice in experiments by Jordan *et al*. [23], led to an even further aggravated hypoglycemia in L-*G6pc*$^{-/-}$ mice (results not shown), similar to rapid changes in blood glucose levels and rebound hypoglycemia that have been observed upon glucose administration in GSD Ia patients [7]. Therefore, we could not assess the effect of glucose on leukocyte changes in L-*G6pc*$^{-/-}$ mice directly. Neutrophils showed a similar response to monocytes in fasted and refed L-*G6pc*$^{-/-}$ mice, although fasting decreased neutrophils by only ~26% (Figure 1G, H, O, P). T- and B-cells were similarly affected (Figure S4A-F), with effects on B-cells being most pronounced.

Collectively, hepatocyte-specific *G6pc1* deficiency decreased circulating leukocytes upon a 6 hour fast, which was restored by refeeding. While all leukocyte populations were affected, we observed major decreases in monocytes, particularly the Ly6C^{hi} population, and also in B-cells.

3.2 Fasting increases plasma corticosterone levels in L-*G6pc*$^{-/-}$ mice

We then sought to elucidate the mechanism causing the decrease in Ly6C^{hi} monocytes in L-*G6pc*$^{-/-}$ mice upon fasting. MCP-1 enhances recruitment of Ly6C^{hi} monocytes from bone marrow by interacting with CCR2 on these cells [36–38]. A previous study has shown that hypoglycemia decreases blood monocytes as a consequence of a reduction in plasma MCP-1 levels [23]. MCP-1 levels in plasma of L-*G6pc*$^{-/-}$ mice were not affected compared to controls after a 6 hour fast (Figure S5A). Also M-CSF was not affected (Figure S5B). We observed a small increase in plasma G-CSF levels (Figures S5C), which cannot explain the fasting-induced reduction in blood

neutrophils in L-*G6pc*$^{-/-}$ mice. We then studied surface markers on monocytes and neutrophils. CCR2, CD11b, and VLA4 expression on Ly6C^{hi} monocytes were not affected in L-*G6pc*$^{-/-}$ mice compared to controls after a 6 hour fast (Figure S5D), as were CXCR4, CD62L, CXCR2 and CD11b on neutrophils (Figure S5E). In sum, hepatocyte-specific *G6pc1* deficiency does not affect surface markers on monocytes and neutrophils upon fasting, suggesting no difference in functionality of these cells.

We then assessed where myeloid cells would accumulate during fasting-induced hypoglycemia in hepatocyte-specific *G6pc1* deficiency. We observed an increase in monocytes in bone marrow in L-*G6pc*$^{-/-}$ mice upon fasting (Figure 2A). While most bone marrow monocytes are Ly6C^{hi}, the Ly6C^{lo} population was increased, perhaps because monocytes lose their Ly6C expression upon retention in the bone marrow. Stem and progenitor cells including LSK cells, CMPs, and GMPs that give rise to myeloid cells were not affected in bone marrow of fasted L-*G6pc*$^{-/-}$ mice (Figure 2B), or in spleen or liver (results not shown). Livers from L-*G6pc*$^{-/-}$ mice showed increased neutrophils (Figure 2C), in line with a previous study where this was attributed to increased hepatic expression of the neutrophil chemoattractant keratinocyte-derived chemokine (KC) that stimulates neutrophil infiltration [39,40]. In sum, the decrease in blood monocytes upon fasting in L-*G6pc*$^{-/-}$ mice may be due to their accumulation in the bone marrow and the decrease in neutrophils due to accumulation in liver.

We then further investigated the mechanism underlying the decrease in blood Ly6C^{hi} monocytes and their accumulation in bone marrow upon fasting-induced hypoglycemia in hepatocyte-specific *G6pc1* deficiency. Hypoglycemia evokes a stress response that leads to increased plasma corticosterone levels in mice [41]. Corticosterone impairs recruitment of monocytes from the bone marrow [42,43]. Bone marrow monocytes are mostly from the Ly6C^{hi} subset [38]. We thus hypothesized that the decrease in Ly6C^{hi} monocytes was due to increased corticosterone levels as a result of hypoglycemia in fasted L-*G6pc*$^{-/-}$ mice. We measured levels of corticosterone and other stress hormones. While fasting increased plasma corticosterone levels in both genotypes, L-*G6pc*$^{-/-}$ mice showed 2-fold higher plasma corticosterone than controls after fasting (Figure 3A). Adrenal gland mass was not affected after a 6 hour fast, likely because the increase in plasma corticosterone was an acute effect (Figure S6). Corticosterone increases the activity of the enzyme phenylethanolamine *N*-methyltransferase (PNMT), which mediates the conversion of

norepinephrine into epinephrine [44]. In line with an increase in corticosterone levels, epinephrine levels were also increased by 2-fold upon fasting in L-*G6pc*$^{-/-}$ mice compared to controls (Figure 3B), while norepinephrine levels were not affected (Figure 3C). Corticosterone and epinephrine have counterregulatory effects on blood monocytes [42,43,45]. Given that we observed a decrease in blood monocytes upon fasting, we hypothesize that the effect of corticosterone on blood monocytes is predominant and investigated this further.

3.3 Inhibition of corticosterone signaling prevents the fasting-induced decrease in blood Ly6C^{hi} monocytes L-*G6pc*$^{-/-}$ mice

We then assessed whether the reduction in Ly6C^{hi} monocytes in fasted L-*G6pc*$^{-/-}$ mice was dependent on the increase in plasma corticosterone levels. We injected mice with the glucocorticoid receptor antagonist mifepristone or vehicle at the start of the fasting period. Strikingly, mifepristone prevented the fasting-induced decrease in total CD45^{+} leukocytes in L-*G6pc*$^{-/-}$ mice completely (Figure 4A). Mifepristone prevented the fasting-induced decrease in Ly6C^{hi} monocytes in L-*G6pc*$^{-/-}$ mice, while effects on other leukocyte populations did not reach statistical significance (Figure 4B, S7). These data confirm our hypothesis that the decrease in Ly6C^{hi} monocytes in fasted L-*G6pc*$^{-/-}$ mice is due to an exaggerated stress response due to elevated plasma corticosterone.

A recent study has shown that hypoglycemia in hepatocyte-specific *G6pc1* deficient mice impairs very-low-density lipoprotein (VLDL) catabolism, which was suggested to be due to decreased lipoprotein lipase (LPL) activity [10]. As a result, plasma triglyceride levels were elevated [10]. Corticosterone may inhibit LPL activity [46,47]. We thus assessed whether the increase in plasma VLDL-triglycerides (VLDL-TG) in fasted L-*G6pc*$^{-/-}$ mice was dependent on plasma corticosterone levels. Mifepristone prevented the increase in plasma VLDL-TG upon fasting in L-*G6pc*$^{-/-}$ mice (Figure S8A, B), suggesting that elevated corticosterone levels contribute to fasting-induced hypertriglyceridemia in GSD Ia.

3.4 Fasting increases bleeding time in L-*G6pc*$^{-/-}$ mice

The increased bleeding tendency in GSD Ia has been attributed to decreases in von Willebrand factor (vWF) [19], disturbed platelet aggregation [16,18], and increased blood pressure [48]. Myeloid cells such as monocytes and neutrophils form leukocyte-platelet aggregates that contribute to coagulation [24]. Hence, a fasting-induced decrease in myeloid cells may reduce the formation of leukocyte-platelet aggregates, impair blood coagulation, and increase bleeding time. To test this hypothesis, we first assessed bleeding time in L-*G6pc*$^{-/-}$ mice in the fed, fasted, non-fasted and refed condition using the tail vein bleeding assay. Similar to observations in GSD Ia patients with poor glycemic control, fasting increased bleeding time in L-*G6pc*$^{-/-}$ mice (Figure 5A). Further confirming these data, L-*G6pc*$^{-/-}$ mice showed an increase in blood loss per minute upon fasting compared to controls (Figure 5B). The increased bleeding time and blood volume loss per minute were restored upon refeeding. Bleeding time and blood volume loss per minute were not affected in the fed and non-fasted state. Collectively, these data show that fasting prolongs bleeding time in L-*G6pc*$^{-/-}$ mice.

We then investigated whether prolonged bleeding time upon fasting was due to a decrease in monocyte-aggregates and neutrophil-aggregates because of a fasting-induced reduction in myeloid cells in L-*G6pc*$^{-/-}$ mice. The percentage of monocytes and neutrophils that formed aggregates with platelets (CD41^{+}) was not affected by hepatocyte-specific *G6pc1* deficiency (Figure S9A, B). This indicates that the capacity of monocytes and neutrophils to form aggregates with platelets did not change under fasting conditions. Nonetheless, the absolute decrease in these cell populations could contribute to less myeloid cell-platelet aggregates and increased bleeding during fasting in hepatocyte-specific *G6pc1* deficiency.

3.5 Fasting does not decrease coagulation factors in L-*G6pc*$^{-/-}$ mice

We next investigated other mechanisms accounting for the fasting-induced increase in bleeding time in L-*G6pc*$^{-/-}$ mice. Since coagulation factors are mainly produced by the liver [49], where *G6pc1* is highly expressed [50], we first assessed whether coagulation factors secreted by the liver and downstream pathways were affected by hepatocyte-specific *G6pc1* deficiency. Prothrombin (PT) time, reflecting the intrinsic coagulation pathway that is dependent on factor VII and the common pathway consisting of factor X, II (thrombin) and I (fibrinogen), was not affected (Figure 6A). Activated partial thromboplastin time (aPTT), reflecting the extrinsic

coagulation pathway dependent on factors XI, XII, VIII and IX, was also not affected (Figure 6B). Plasma levels of coagulation factors V (FV) and VIII (FVIII) were increased in L-*G6pc*$^{-/-}$ mice in the fed and fasted condition, while factor VII (FVII) was not affected (Figure 6C-E). Given that the increases in FV and FVIII would result in an increase in coagulation, these increases are unlikely to explain the bleeding phenotype of L-*G6pc*$^{-/-}$ mice. It has been described that GSD Ia patients show decreased vWF levels [19]. On the contrary, we found that L-*G6pc*$^{-/-}$ mice showed increased vWF levels upon fasting (Figure 6F). The increase in plasma vWF and FVIII could be the consequence of the fasting-induced increase in plasma corticosterone [51–53]. Similar to FV and FVIII, vWF would increase coagulation. Therefore, these increases cannot explain the prolonged bleeding phenotype in fasted L-*G6pc*$^{-/-}$ mice. Hence, the bleeding phenotype in L-*G6pc*$^{-/-}$ mice upon fasting is not due to decreases in vWF, FVIII or coagulation factors produced by the liver.

3.6 Fasting disturbs platelet aggregation in L-*G6pc*$^{-/-}$ mice

Even though the number of patients was limited (between 2 and 7 per study), it has been reported that GSD Ia patients show disturbed platelet aggregation [16–18]. This could account for the prolonged bleeding time in GSD Ia. We thus assessed whether fasting affected platelet aggregation in L-*G6pc*$^{-/-}$ mice. While blood platelet counts were not different between genotypes in both the fed and fasted condition (Figure 7A), studies on platelet function did reveal distinct differences. Initially, ADP-induced stimulation of platelet rich plasma from both controls and L-*G6pc*$^{-/-}$ mice led to aggregation in both the fed and fasted condition (Figure 7B). Strikingly, after maximum aggregation had been reached, platelets isolated from fasted, but not from non-fasted L-*G6pc*$^{-/-}$ mice, showed ~50% platelet disaggregation (Figure 7B, C). Hence, hepatocyte-specific *G6pc1* deficiency disturbs platelet aggregation after fasting. Among all mechanisms that we have explored, it is most likely that disturbed platelet aggregation accounts for the prolonged bleeding time in L-*G6pc*$^{-/-}$ mice. We anticipate that this is also the main mechanism accounting for the bleeding tendency observed in hypoglycemic GSD Ia patients.

4. Discussion

Our findings show that hepatocyte-specific *G6pc1* deficiency in mice increases plasma corticosterone levels, decreases blood leukocytes, and disturbs platelet aggregation upon fasting. These results are most likely the consequence of fasting-induced hypoglycemia. The fasting-induced decrease in leukocytes in hepatocyte-specific *G6pc1* deficiency was mainly reflected by a decrease in Ly6C^{hi} monocytes and was prevented by the glucocorticoid receptor antagonist mifepristone. Furthermore, we found that hepatocyte-specific *G6pc1* deficiency prolonged bleeding time upon fasting due to disturbed platelet aggregation. While previous studies have shown a relationship between hyperglycemia and monocytosis [54], our data indicate a similar relationship under conditions of fasting-induced hypoglycemia in hepatocyte-specific *G6pc1* deficiency, reflected by decreases in blood monocyte levels and disturbed platelet aggregation.

A relationship between glucose levels and blood monocytes in the setting of transient intermittent hyperglycemia independent of diabetes, and prolonged fasting has been shown previously [54]. Four injections of glucose over a period of 6 hours increase blood monocyte levels, in particular the Ly6C^{hi} population, in wild-type mice [54], and a fasting period of 20 hours decreases blood monocytes in wild-type mice, with reversal by glucose administration [23]. Similarly, a 19 hour fasting period in humans decreases plasma glucose levels and blood monocytes [23]. Several studies thus show a positive relationship between blood monocytes and plasma glucose levels [23,54], sharing similarities with our observations in a mouse model of hepatic GSD Ia.

While transient intermittent hyperglycemia increases blood monocytes due to elevated S100A8/A9 secretion by neutrophils as a consequence of glucose transporter (GLUT)-1 mediated glucose uptake [54], the decrease in blood monocytes upon hypoglycemia during prolonged fasting is considered to be secondary to a decrease in MCP-1 [23]. MCP-1 interacts with its receptor CCR2 on bone marrow monocytes to promote their egress from bone marrow into blood [36–38]. We did not find differences in plasma MCP-1 upon fasting-induced hypoglycemia in hepatocyte-specific *G6pc1* deficiency, but we did observe an increase in plasma corticosterone and epinephrine. While corticosterone decreases blood monocytes, epinephrine has the opposite effect [45]. In diabetes, injections of insulin increase epinephrine levels [55] and blood monocytes [45], and presumably as a result thereof, patients with type 2 diabetes show high levels of blood monocytes [22], although hyperglycemia also contributes to this effect [22].

Nonetheless, the question remains as to why monocytes were not increased as a consequence of the increased epinephrine in mice with hepatocyte-specific *G6pc1* deficiency, similar to effects of insulin injections in patients with diabetes. We think this relates to diabetic patients having impaired adrenocorticotrophic hormone responses to hypoglycemia, leading to suppression of cortisol production by the adrenal gland [56]. As such, cortisol levels are not upregulated during hypoglycemia as a consequence of insulin injections [56], while epinephrine levels do increase, leading to elevated blood monocyte levels. Our studies show that fasting-induced hypoglycemia in hepatocyte-specific *G6pc1* deficiency increases plasma levels of both corticosterone and epinephrine, and the decrease in blood monocytes suggests that the effect of corticosterone is predominant. Indeed, we found that the corticosterone receptor antagonist mifepristone reversed the fasting-induced decrease in Ly6C^{hi} monocytes in L-*G6pc*$^{-/-}$ mice. We mainly observed differences in the Ly6C^{hi} monocyte subset, presumably because corticosterone impairs the egress of monocytes from the bone marrow [42,43,57], and most bone marrow monocytes are Ly6C^{hi} [38]. This is consistent with previous studies in rats showing that acute stress or administration of corticosterone decreases blood monocytes within 2 hours [42,58]. B-cells were also reduced by fasting in L-*G6pc*$^{-/-}$ mice. Previous studies have shown that blood B-cell levels are controlled by corticosterone, at least when corticosterone levels are elevated for a long period of time (72 hours) [59]. Mifepristone tended to reverse the decrease in B-cells in L-*G6pc*$^{-/-}$ mice, although this did not reach statistical significance. Previous studies have also shown that myocardial infarction (MI) leads to activation of the sympathetic nervous system, increasing norepinephrine production which acts on β_3-adrenoceptors in bone marrow and promotes stem cell mobilization within 48 hours of MI [60]. We did not observe any differences in norepinephrine levels or on hematopoietic stem and progenitor cells in the bone marrow, indicating that this mechanism did not play a role in L-*G6pc*$^{-/-}$ mice.

GSD Ia patients display elevated levels of cortisol, the human homologue of corticosterone [61]. This was observed in the fed state, under conditions of good glycemic control. This effect was attributed to production of NADPH in hepatocytes resulting from G6P accumulation. NADPH is a co-factor required for 11β-HSD1 reductase activity [62], resulting in conversion of inactive glucocorticoids (cortisone in humans and 11-dehydrocortisone in mice) into active glucocorticoids (cortisol and corticosterone in humans and mice, respectively) [63]. GSD Ia patients show increased conversion of administered cortisone into cortisol after overnight

dexamethasone suppression [62], consistent with increased 11β-HSD1 reductase activity and elevated plasma cortisol levels [61]. Although L-*G6pc*$^{-/-}$ mice do accumulate G6P in the liver, 11β-HSD1 reductase activity was not affected [62]. This is likely the consequence of 11β-HSD1 reductase activity being 20 times higher in mice than in humans [62,64], and may explain why plasma corticosterone is not elevated in L-*G6pc*$^{-/-}$ mice in the fed state.

The increase in plasma cortisol in the fed state does not exclude that GSD Ia patients may show high cortisol levels upon fasting-induced hypoglycemia, similar to mice with hepatocyte-specific *G6pc1* deficiency. Hypoglycemia in GSD Ia patients correlates with hyperlipidemia, in particular increased VLDL-TGs [7,10,65,66]. Cortisol increases VLDL-TG plasma levels [67,68]. We found that the glucocorticoid receptor antagonist mifepristone suppressed the fasting-induced increase in plasma VLDL-TG in L-*G6pc*$^{-/-}$ mice, consistent with a role for this antagonist in promoting VLDL-TG clearance, as suggested [69]. These data indicate that increased plasma cortisol due to poor glycemic control contributes to high plasma VLDL-TG levels in GSD Ia patients [46,47].

Despite elevated VLDL-TG levels, a study in 9 GSD Ia patients has shown that carotid intima media thickness was not increased in GSD Ia patients compared to controls [15]. While this effect may be explained by VLDL particles being too large to enter the vessel wall, similar to a setting of *Apolipoprotein C3* overexpression in mice [70], our data show that in a setting of poor glycemic control, levels of blood pro-inflammatory Ly6C^{hi} monocytes are decreased. Ly6C^{hi} monocytes infiltrate into atherosclerotic lesions [71]. Monocytosis enhances atherosclerosis, as shown by studies in animal models [71] and humans [72]. The outcome of our studies suggests that conditions of poor glycemic control in GSD Ia patients may reduce the levels of pro-inflammatory monocytes. This could contribute to the decrease in atherosclerosis in GSD Ia.

We also found that fasted L-*G6pc*$^{-/-}$ mice show prolonged bleeding time in the tail vein bleeding assay, replicating the enhanced bleeding tendency in GSD Ia patients with poor glycemic control [16–18]. Various mechanisms have been proposed for this observation, including decreases in vWF [19], disturbed platelet aggregation [16,18], and increased blood pressure [48]. Because GSD Ia is a rare disorder, studies typically include small numbers of patients (between 2 and 7 per study), and hence the bleeding phenotype in GSD Ia has not been evaluated systematically. We found that some coagulation factors secreted by the liver, one of the main organs affected in

GSD Ia, were increased in L-*G6pc*$^{-/-}$ mice upon fasting, as were FVIII and vWF; however, these increases would rather have led to increased coagulation and thus cannot explain the bleeding phenotype in GSD Ia. Strikingly, we observed that, only in the fasted condition, L-*G6pc*$^{-/-}$ mice showed disturbed platelet aggregation. This was reflected by ~50% platelet disaggregation in response to ADP after maximum aggregation had been reached. This indicates that the secondary wave of platelet aggregation, which is dependent on the release of ADP and ATP stored in the dense granules of platelets [73,74], is absent in hepatocyte-specific *G6pc1* deficiency. Therefore, the platelet activation process and recruitment of platelets cannot be amplified and a solid platelet plug cannot be formed [73–76]. This is commonly observed in patients with dense granule storage pool disease [77], which is characterized by an almost complete absence of dense granule ADP and ATP [78,79] and a bleeding phenotype [79]. In line with these observations, it has been reported that platelets of 2 GSD Ia patients contained less ADP and ATP during hypoglycemia [18]. Continuous gastric drip feeding to maintain normoglycemia corrected ADP and ATP levels as well as the disturbed platelet aggregation phenotype [18]. Together with our results in mice with hepatocyte-specific *G6pc1* deficiency, these findings indicate that disturbed platelet aggregation in GSD Ia is the consequence of low levels of ATP and ADP in the platelet dense granules due to hypoglycemia. In addition, we cannot exclude that the decrease in myeloid cells in L-*G6pc*$^{-/-}$ mice may have led to a decrease in absolute numbers of monocyte- and neutrophil-platelet aggregates, which could contribute to increased bleeding in fasted L-*G6pc*$^{-/-}$ mice compared to controls.

Several studies have shown that glucose levels affect platelet aggregation. Platelet deficiency of GLUT 1 and GLUT 3, which mediate glucose uptake, decreases platelet activation in response to protease-activated receptor 4 peptide (PAR4) and prolongs bleeding time in mice [80,81]. These observations support our finding that bleeding time is increased in fasting-induced hypoglycemia in L-*G6pc*$^{-/-}$ mice. However, in contrast to findings in GSD Ia [16–18], acute hypoglycemia during an insulin stress test in humans increases platelet aggregation in response to ADP without affecting platelet ATP and ADP content [82]. The exact mechanism for this finding is unclear. Furthermore, acute insulin-induced hypoglycemia has been shown to increase vWF levels in humans [83,84], likely the consequence of the hypoglycemia-induced increase in corticosterone levels [51,52] or endothelial dysfunction [84,85], and enhancing platelet aggregation. In sum,

several mechanisms affecting platelet aggregation or disaggregation, including the one identified in GSD Ia, are regulated by blood glucose levels.

A limitation of our study is the use of adult, hepatocyte-specific *G6pc1* deficient mice. Whole body *G6pc1*$^{-/-}$ mice require daily glucose injections to survive, rarely live longer than 3 months, and cannot be used to investigate the effects of *G6pc1* deficiency during fasting [11,86,87]. Although kidney-specific and intestinal-specific *G6pc1* deficient mice do not become hypoglycemic upon fasting [88–90], we cannot exclude that in GSD Ia patients loss of G6pc activity in kidney and intestine contributes to the bleeding phenotype under conditions of poor glycemic control.

5. Conclusion

We have shown that hepatocyte-specific *G6pc1* deficiency increases plasma corticosterone levels upon fasting, which decreases Ly6C^{hi} monocytes in blood. Although direct effects of poor glycemic control on cortisol or leukocyte levels have not been evaluated in GSD Ia patients, this would be of interest, especially given that increased plasma cortisol may contribute to elevated VLDL-TG under conditions of poor glycemic control in GSD Ia. In addition, we found that hepatocyte-specific *G6pc1* deficiency disturbs platelet aggregation during fasting-induced hypoglycemia, accounting for the bleeding phenotype in GSD Ia. Together, these results highlight the clinical necessity of maintaining good glycemic control in GSD Ia.

CRediT author statement

Anouk M. La Rose: Conceptualization, Methodology, Investigation, Writing – Original Draft preparation. Venetia Bazioti, Joanne A. Hoogerland, Arthur F. Svendsen, Anouk G. Groenen, Martijn van Faassen, Martijn G.S. Rutten, Niels J. Kloosterhuis, Bertien Dethmers-Ausema, J. Hendrik Nijland: Investigation. G. Mithieux, F. Rajas: Resources, Writing – Review & Editing. M.V. Lukens, F. Kuipers, O. Soehnlein, M.H. Oosterveer: Conceptualization, Writing – Review & Editing. M. Westerterp: Conceptualization, Methodology, Investigation, Writing – Review & Editing, Supervision, Funding Acquisition.

Acknowledgements

The authors thank Vincent Bloks for his help on the hepatic coagulation factor analysis. M.H. Oosterveer and M. Westerterp are both supported by VIDI grants (917.17.373 and 917.15.350, respectively) from the Netherlands Organization of Scientific Research, and Rosalind Franklin Fellowships from the University of Groningen.

References

[1] Chou JY, Jun HS, Mansfield BC. Type I glycogen storage diseases: disorders of the glucose-6-phosphatase/glucose-6-phosphate transporter complexes. J Inherit Metab Dis 2015;38:511–9.

[2] Lei KJ, Shelly LL, Pan CJ, Sidbury JB, Chou JY. Mutations in the glucose-6-phosphatase gene that cause glycogen storage disease type 1a. Science 1993;262:580–3.

[3] Lei KJ, Chen YT, Chen H, Wong LJC, Liu JL, McConkie-Rosell A, et al. Genetic basis of glycogen storage disease type 1a: Prevalent mutations at the glucose-6-phosphatase locus. Am J Hum Genet 1995;57:766–71.

[4] Chevalier-Porst F, Bozon D, Bonardot AM, Bruni N, Mithieux G, Mathieu M, et al. Mutation analysis in 24 French patients with glycogen storage disease type la. J Med Genet 1996;33:358–60.

[5] Chou JY, Kim G-Y, Cho J-H. Recent development and gene therapy for glycogen storage disease type Ia. Liver Res 2017;1:174–80.

[6] Dambska M, Labrador EB, Kuo CL, Weinstein DA. Prevention of complications in glycogen storage disease type Ia with optimization of metabolic control. Pediatr Diabetes 2017;18:327–31.

[7] Rake JP, Visser G, Labrune P, Leonard J V, Ullrich K, Smit GPA, et al. Guidelines for management of glycogen storage disease type I - European Study on Glycogen Storage Disease Type I (ESGSD I). Eur J Pediatr 2002;161:S112-119.

[8] Carvalho PMS, Silva NJMM, Dias PGD, Porto JFC, Santos LC, Costa JMN. Glycogen Storage Disease type 1a - a secondary cause for hyperlipidemia: report of five cases. J Diabetes Metab Disord 2013;12:25.

[9] Rake JP, Visser G, Labrune P, Leonard JV, Ullrich K, Smit GP. Glycogen storage disease type I : diagnosis, management, clinical course and outcome. Results of the European Study on Glycogen Storage Disease Type I (ESGSD I). Eur J Pediatr 2002;161:S20-34.

[10] Hoogerland JA, Peeks F, Hijmans B., Wolters JC, Kooijman S, Bos T, et al. Impaired VLDL catabolism links hypoglycemia to hypertriglyceridemia in GSDIa. J Inherit Metab

Dis 2021;Epub ahead of print.

[11] Lei K, Chen H, Pan C, Ward JM, Mosinger B, Lee EJ, et al. Glucose-6-phosphatase dependent substrate transport in the glycogen storage disease type-1a mouse. Nat Genet 1996;13:203–9.

[12] Lei Y, Hoogerland JA, Bloks VW, Bos T, Bleeker A, Wolters H, et al. Hepatic Carbohydrate Response Element Binding Protein Activation Limits Nonalcoholic Fatty Liver Disease Development in a Mouse Model for Glycogen Storage Disease Type 1a. Hepatology 2020;72:1638–53.

[13] Wang D, Fiske L, Carreras C, Weinstein D. Natural history of hepatorcellular adenoma formation in glycogen storage disease type I. J Pediatr 2011;159:442–6.

[14] Beegle RD, Brown LM, Weinstein DA. Regression of Hepatocellular Adenomas with Strict Dietary Therapy in Patients with Glycogen Storage Disease Type I. JIMD Rep 2015;18:23–32.

[15] Ubels F, Rake J, Smit P, Smit A, Slaets J. Is glycogen storage disease 1a associated with atherosclerosis? Eur J Pediatr 2002;161:S62–4.

[16] Czapek EE, Deykin D, Salzman EW. Platelet dysfunction in glycogen storage disease type I. Blood 1973;41:235–47.

[17] Corby DG, Putnam CW, Greene HL. Impaired platelet function in glucose-6-phosphatase deficiency. J Pediatr 1974;85:71–6.

[18] Hutton RA, Macnab AJ, Rivers RPA. Defect of platelet function associated with chronic hypoglycaemia. Arch Dis Child 1976;51:49–55.

[19] Mühlhausen C, Schneppenheim R, Budde U, Merkel M, Muschol N, Ullrich K, et al. Decreased plasma concentration of von Willebrand factor antigen (VWF:Ag) in patients with glycogen storage disease type Ia. J Inherit Metab Dis 2005;28:945–50.

[20] Bandsma RHJ, Rake JP, Visser G, Neese RA, Hellerstein MK, Van Duyvenvoorde W, et al. Increased lipogenesis and resistance of lipoproteins to oxidative modification in two patients with glycogen storage disease type 1a. J Pediatr 2002;140:256–60.

[21] Peeks F, Steunenberg TAH, de Boer F, Rubio-gozalbo ME, Williams M, Burghard R, et al. Clinical and biochemical heterogeneity between patients with glycogen storage disease type IA : the added value of CUSUM for metabolic control. J Inherit Metab Dis 2017;40:695–702.

[22] Nagareddy PR, Murphy AJ, Stirzaker RA, Hu Y, Yu S, Miller RG, et al. Hyperglycemia promotes myelopoiesis and impairs the resolution of atherosclerosis. Cell Metab 2013;17:695–708.

[23] Jordan S, Tung N, Casanova-Acebes M, Chang C, Cantoni C, Zhang D, et al. Dietary Intake Regulates the Circulating Inflammatory Monocyte Pool. Cell 2019;178:1102-1114.e17.

[24] Mansour A, Roussel M, Gaussem P, Nédelec-Gac F, Pontis A, Flécher E, et al. Platelet Functions During Extracorporeal Membrane Oxygenation. Platelet–Leukocyte Aggregates Analyzed by Flow Cytometry as a Promising Tool to Monitor Platelet Activation. J Clin Med 2020;9:2361.

[25] Celi A, Pellegrini G, Lorenzet R, De Blasi A, Ready N, Furie BC, et al. P-selectin induces the expression of tissue factor on monocytes. Proc Natl Acad Sci U S A 1994;91:8767–71.

[26] Kraakman MJ, Lee MKS, Al-Sharea A, Dragoljevic D, Barrett TJ, Montenont E, et al. Neutrophil-derived S100 calcium-binding proteins A8/A9 promote reticulated thrombocytosis and atherogenesis in diabetes. J Clin Invest 2017;127:2133–47.

[27] Mutel E, Abdul-Wahed A, Ramamonjisoa N, Stefanutti A, Houberdon I, Cavassila S, et al. Targeted deletion of liver glucose-6 phosphatase mimics glycogen storage disease type 1a including development of multiple adenomas. J Hepatol 2011;54:529–37.

[28] Hawley JM, Owen LJ, Mackenzie F, Mussell C, Cowen S, Keevil BG. Candidate reference measurement procedure for the quantification of total serum cortisol with LC-MS/MS. Clin Chem 2016;62:262–9.

[29] van Faassen M, Bischoff R, Eijkelenkamp K, de Jong WHA, van der Ley CP, Kema IP. In Matrix Derivatization Combined with LC-MS/MS Results in Ultrasensitive Quantification of Plasma Free Metanephrines and Catecholamines. Anal Chem 2020;92:9072–8.

[30] Liu Y, Jennings NL, Dart AM, Du X-J. Standardizing a simpler, more sensitive and accurate tail bleeding assay in mice. World J Exp Med 2012;2:30–6.

[31] Hoogerland JA, Lei Y, Wolters JC, de Boer JF, Bos T, Bleeker A, et al. Glucose-6-Phosphate Regulates Hepatic Bile Acid Synthesis in Mice. Hepatology 2019;70:2171–84.

[32] Romano A, Mackie A, Farina F, Aponte M, Sarghini F, Masi P. Characterisation, in vitro digestibility and expected glycemic index of commercial starches as uncooked ingredients. J Food Sci Technol 2016;53:4126–34.

[33] Casanova-Acebes M, Pitaval C, Weiss LA, Nombela-Arrieta C, Chèvre R, A-González N, et al. Rhythmic modulation of the hematopoietic niche through neutrophil clearance. Cell 2013;153:1025–35.

[34] Murphy AJ, Akhtari M, Tolani S, Pagler T, Bijl N, Kuo C, et al. ApoE regulates hematopoeitic stem cell proliferation, monocytosis, and monocyte accumulation in atherosclerotic lesions in mice. J Clin Invest 2011;121:4138–49.

[35] Jensen TL, Kiersgaard MK, Sørensen DB, Mikkelsen LF. Fasting of mice: A review. Lab Anim 2013;47:225–40.

[36] Serbina N V, Pamer EG. Monocyte emigration from bone marrow during bacterial infection requires signals mediated by chemokine receptor CCR2. Nat Immunol 2006;7:311–7.

[37] Combadière C, Potteaux S, Rodero M, Simon T, Pezard A, Esposito B, et al. Combined inhibition of CCL2, CX3CR1, and CCR5 abrogates Ly6Chi and Ly6Clo monocytosis and almost abolishes atherosclerosis in hypercholesterolemic mice. Circulation 2008;117:1649–57.

[38] Tsou C-L, Peters W, Si Y, Slaymaker S, Aslanian AM, Weisberg SP, et al. Critical roles for CCR2 and MCP-3 in monocyte mobilization from bone marrow and recruitment to inflammatory sites. J Clin Invest 2007;117:902–9.

[39] Kim SY, Chen LY, Yiu WH, Weinstein DA, Chou JY. Neutrophilia and elevated serum cytokines are implicated in glycogen storage disease type Ia. FEBS Lett 2007;581:3833–8.

[40] Kim SY, Weinstein DA, Starost MF, Mansfield BC, Chou JY. Necrotic foci, elevated chemokines and infiltrating neutrophils in the liver of glycogen storage disease type Ia. J Hepatol 2008;48:479–85.

[41] Shum K, Inouye K, Chan O, Mathoo J, Bilinski D, Matthews SG, et al. Effects of antecedent hypoglycemia, hyperinsulinemia, and excess corticosterone on hypoglycemic counterregulation. Am J Physiol Endocrinol Metab 2001;281:455–65.

[42] Dhabhar FS, Miller AH, McEwen BS, Spencer RL. Effects of stress on immune cell distribution: Dynamics and hormonal mechanisms. J Immunol 1995;154:5511–27.

[43] Thompson J, van Furth R. The effect of glucocorticosteroids on the proliferation and kinetics of promonocytes and monocytes of the bone marrow. J Exp Med 1973;137:10–21.

[44] Wurtman RJ, Axelrod J. Adrenaline synthesis: control by the pituitary gland and adrenal glucocorticoids. Science 1965;150:1464–5.

[45] Dimitrov S, Lange T, Born J. Selective Mobilization of Cytotoxic Leukocytes by Epinephrine. J Immunol 2010;184:503–11.

[46] Koliwad SK, Kuo T, Shipp LE, Gray NE, Backhed F, So AYL, et al. Angiopoietin-like 4 (ANGPTL4, fasting-induced adipose factor) is a direct glucocorticoid receptor target and participates in glucocorticoid-regulated triglyceride metabolism. J Biol Chem 2009;284:25593–601.

[47] Dijk W, Kersten S. Regulation of lipoprotein lipase by Angptl4. Trends Endocrinol Metab 2014;25:146–55.

[48] Yetman RJ, Andrew-Casal M, Hermida RC, Dominguez BW, Portman RJ, Northrup H, et al. Circadian pattern of blood pressure, heart rate, and double product in liver glycogen storage disease. Chronobiol Int 2002;19:765–83.

[49] Kujovich JL. Coagulopathy in liver disease: a balancing act. Hematol Am Soc Hematol Educ Progr 2015:243–9.

[50] Gjorgjieva M, Mithieux G, Rajas F. Hepatic stress associated with pathologies characterized by disturbed glucose production. Cell Stress 2019;3:86–99.

[51] Majoor CJ, Sneeboer MMS, de Kievit A, Meijers JCM, van der Poll T, Lutter R, et al. The influence of corticosteroids on hemostasis in healthy subjects. J Thromb Haemost 2016;14:716–23.

[52] Von Känel R, Dimsdale JE. Effects of sympathetic activation by adrenergic infusions on hemostasis in vivo. Eur J Haematol 2000;65:357–69.

[53] Dal Bo Zanon R, Fornasiero L, Boscaro M, Cappellato G, Fabris F, Girolami A. Increased factor VIII associated activities in Cushing's syndrome: A probable hypercoagulable state. Thromb Haemost 1982;47:116–7.

[54] Flynn MC, Kraakman MJ, Tikellis C, Lee MKS, Hanssen NMJ, Kammoun HL, et al. Transient Intermittent Hyperglycemia Accelerates Atherosclerosis by Promoting Myelopoiesis. Circ Res 2020;127:877–92.

[55] Jin WL, Azuma K, Mita T, Goto H, Kanazawa A, Shimizu T, et al. Repetitive hypoglycaemia increases serum adrenaline and induces monocyte adhesion to the endothelium in rat thoracic aorta. Diabetologia 2011;54:1921–9.

[56] Rhyu YA, Jang JY, Park S, An JH, Kim DL, Kim SK, et al. Impaired cortisol and growth hormone counterregulatory responses among severe hypoglycemic patients with type 2 diabetes mellitus. Endocrinol Metab 2019;34:187–94.

[57] Thompson J, van Furth R. The effect of glucocorticosteroids on the kinetics of mononuclear phagocytes. J Exp Med 1970;131:429–42.

[58] Dhabhar FS, Malarkey WB, Neri E, McEwen BS. Stress-induced redistribution of immune cells-From barracks to boulevards to battlefields: A tale of three hormones. Psychoneuroendocrinology 2012;37:1345–68.

[59] Courties G, Frodermann V, Honold L, Zheng Y, Herisson FE, Schloss MJ, et al. Glucocorticoids Regulate Bone Marrow B Lymphopoiesis After Stroke. Circ Res 2019;124:1372–85.

[60] Dutta P, Courties G, Wei Y, Leuschner F, Gorbatov R, Robbins CS, et al. Myocardial infarction accelerates atherosclerosis. Nature 2012;487:325–9.

[61] Rossi A, Simeoli C, Salerno M, Ferrigno R, Della Casa R, Colao A, et al. Imbalanced cortisol concentrations in glycogen storage disease type I: Evidence for a possible link between endocrine regulation and metabolic derangement. Orphanet J Rare Dis 2020;15:1–8.

[62] Walker EA, Ahmed A, Lavery GG, Tomlinson JW, So YK, Cooper MS, et al. 11β-Hydroxysteroid dehydrogenase type 1 regulation by intracellular glucose 6-phosphate provides evidence for a novel link between glucose metabolism and hypothalamo-pituitary-adrenal axis function. J Biol Chem 2007;282:27030–6.

[63] Tomlinson JW, Walker EA, Bujalska IJ, Draper N, Lavery GG, Cooper MS, et al. 11β-Hydroxysteroid dehydrogenase type 1: A tissue-specific regulator of glucocorticoid response. Endocr Rev 2004;25:831–66.

[64] Lavery GG, Walker EA, Draper N, Jeyasuria P, Marcos J, Shackleton CHL, et al. Hexose-6-phosphate dehydrogenase knock-out mice lack 11β- hydroxysteroid dehydrogenase type 1-mediated glucocorticoid generation. J Biol Chem 2006;281:6546–51.

[65] Derks TGJ, van Rijn M. Lipids in hepatic glycogen storage diseases: pathophysiology, monitoring of dietary management and future directions. J Inherit Metab Dis 2015;38:537–43.

[66] Kishnani PS, Austin SL, Abdenur JE, Arn P, Bali DS, Boney A, et al. Diagnosis and management of glycogen storage disease type I: A practice guideline of the American College of Medical Genetics and Genomics. Genet Med 2014;16:1–29.

[67] Klausner H, Heimberg M. Effect of adrenalcortical hormones on release of triglycerides and glucose by liver. Am J Physiol 1967;212:1236–46.

[68] Arnaldi G, Scandali VM, Trementino L, Cardinaletti M, Appolloni G, Boscaro M. Pathophysiology of dyslipidemia in Cushing's syndrome. Neuroendocrinology 2010;92:86–90.

[69] Kroon J, Koorneef LL, Van Den Heuvel JK, Verzijl CRC, Van De Velde NM, Mol IM, et al. Selective glucocorticoid receptor antagonist CORT125281 activates brown adipose tissue and alters lipid distribution in male mice. Endocrinology 2018;159:535–46.

[70] Ebara T, Ramakrishnan R, Steiner G, Shachter NS. Chylomicronemia due to Apolipoprotein CIII Overexpression in Apolipoprotein E-null Mice Apolipoprotein CIII – induced Hypertriglyceridemia Is Not Mediated by Effects on Apolipoprotein E. J Clin Invest 1997;99:2672–81.

[71] Swirski FK, Libby P, Aikawa E, Alcaide P, Luscinskas FW, Weissleder R, et al. Ly-6Chi monocytes dominate hypercholesterolemia-associated monocytosis and give rise to macrophages in atheromata. J Clin Invest 2007;117:195–205.

[72] Coller BS. Leukocytosis and Ischemic Vascular Disease Morbidity and Mortality Is It Time to Intervene ? ATVB 2005;25:658–70.

[73] Erhardt JA, Pillarisetti K TJ. Potentiation of platelet activation through the stimulation of P2X 1 receptors. J Thromb Haemost 2003;1:2626–35.

[74] Hoylaerts MF, Oury C, Toth-zsamboki E, Vermylen J, Hoylaerts MF, Toth-zsamboki E, et al. ADP receptors in platelet activation and aggregation ADP receptors in platelet activation and aggregation. Platelets 2000;11:307–9.

[75] Daniel JL, Dangelmaier C, Jin J, Ashby B, Smith JB, Kunapuli SP. Molecular Basis for ADP-induced Platelet Activation. J Biol Chem 1998;273:2024–9.

[76] Jiang L, Xu C, Yu S, Liu P, Luo D, Zhou Q, Gao C HH. A critical role of thrombin / PAR-1 in ADP-induced platelet secretion and the second wave of aggregation. J Thromb Haemost 2013;11:930–40.

[77] Weiss HJ LB. The response of platelets to epinephrine in storage pool deficiency - evidence pertaining to the role of ADP in mediating primary and secondary aggregation. Blood 1988;72:1717–25.

[78] Dupuis A, Bordet J, Eckly A, Gachet C. Platelet δ -Storage Pool Disease : An Update. J Clin Med 2020;9:2508.

[79] Pareti FI, Day HJ, Mills DCB. Nucleotide and Serotonin Metabolism in Platelets With Defective Secondary Aggregation. Blood 1974;44:789–800.

[80] Fidler TP, Campbell RA, Funari T, Chaudhuri D, Weyrich AS, Abel ED, et al. Deletion of

GLUT1 and GLUT3 Reveals Multiple Roles for Glucose Metabolism in Platelet and Megakaryocyte Function Article Deletion of GLUT1 and GLUT3 Reveals Multiple Roles for Glucose Metabolism in Platelet and Megakaryocyte Function. Cell Rep 2017;20:881–94.

[81] Fidler TP, Marti A, Gerth K, Middleton EA, Campbell RA, Rondina MT, et al. Glucose Metabolism Is Required for Platelet Hyperactivation in a Murine Model of Type 1 Diabetes. Diabetes 2019;68:932–8.

[82] Hutton RA, Mikhailidis D, Dormandy KM, Ginsburg J. Platelet aggregation studies during transient hypoglycaemia. A potential method for evaluating platelet function. J Clin Pathol 1979;32:434–8.

[83] Fisher BM, Quin JD, Rumley A, Lennie SE, Small M, MacCuish AC LG. Effects of acute insulin-induced hypoglycaemia on haemostasis, fibrinolysis and haemorheology in insulin-dependent diabetic patients and control subjects. Clin Sci 1991;80:525–31.

[84] Wright RJ, Newby DE, Stirling D, Ludlam CA, Macdonald IA, Frier BM. Effects of Acute Insulin-Induced Hypoglycemia on Indices of Inflammation. Diabetes Care 2010;33:1591–7.

[85] Lip GYH, Blann A. von Willebrand factor: A marker of endothelial dysfunction in vascular disorders? Cardiovasc Res 1997;34:255–65.

[86] Yiu WH, Lee YM, Peng WT, Pan CJ, Mead PA, Mansfield BC, et al. Complete normalization of hepatic G6PC deficiency in murine glycogen storage disease type Ia using gene therapy. Mol Ther 2010;18:1076–84.

[87] Salganik S V., Weinstein DA, Shupe TD, Salganik M, Pintilie DG, Petersen BE. A detailed characterization of the adult mouse model of glycogen storage disease Ia. Lab Investig 2009;89:1032–42.

[88] Clar J, Gri B, Calderaro J, Birling MC, Hérault Y, Smit GPA, et al. Targeted deletion of kidney glucose-6 phosphatase leads to nephropathy. Kidney Int 2014;86:747–56.

[89] Soty M, Penhoat A, Amigo-Correig M, Vinera J, Sardella A, Vullin-Bouilloux F, et al. A gut-brain neural circuit controlled by intestinal gluconeogenesis is crucial in metabolic

health. Mol Metab 2015;4:106–17.

[90] Penhoat A, Fayard L, Stefanutti A, Mithieux G, Rajas F. Intestinal gluconeogenesis is crucial to maintain a physiological fasting glycemia in the absence of hepatic glucose production in mice. Metabolism 2014;63:104–11.

Figure legends

Figure 1. Fasting decreases blood monocytes and neutrophils in L-*G6pc*$^{-/-}$ mice. Hepatocyte-specific *G6pc1* deficiency was induced by tamoxifen injections. Over a period of 6-16 weeks after tamoxifen injections, blood glucose and leukocyte levels were assessed at Zeitgeber Time (ZT) 1 (fed), ZT7 (6 hour fast during the inactive period or non-fasted), and, in case of fasting, the next morning at ZT1 (refeeding during the inactive and active period). For each experiment, the same mouse was measured in the fed (ZT1) and fasted (ZT7) or non-fasted (ZT7) condition, and in case of fasting, in the refed condition (ZT1, the next morning). (**A-B**) Blood glucose levels. (**C-D**) Total CD45^{+} leukocyte levels. (**E-H**) Representative flow cytometry plots of monocyte and neutrophils as percentage of CD45^{+} leukocytes. Monocyte subsets are shown in the fed (**E-F**) and fasted (**G-H**) condition. Neu denotes neutrophils. (**I-P**) Quantification of total monocytes, monocyte subsets and neutrophils in the fed, fasted or non-fasted, and refed condition. (n= 12-16). Data are shown as mean ± SEM. *p<0.05, **p<0.01, ***p<0.001 by t-test. Experiments have been repeated 6 times with similar results.

Figure 2. Fasting increases bone marrow monocytes and hepatic neutrophils in L-*G6pc*$^{-/-}$ mice. Hepatocyte-specific *G6pc1* deficiency was induced by tamoxifen injections. Sixteen weeks after tamoxifen injections, (**A**) total monocytes, Ly6C^{lo} and Ly6C^{hi} monocyte subsets and neutrophils in bone marrow (BM) were assessed by flow cytometry after a 6 hour fast. (**B**) Lin^{-}, Sca1^{+}, cKit^{+} (LSK) cells, common myeloid progenitors (CMP) and granulocyte/monocyte progenitors (GMP) in the bone marrow were assessed by flow cytometry after a 6 hour fast. (**C**) Total monocytes and neutrophils were assessed in liver after a 6 hour fast. Data are shown as mean ± SEM. *p<0.05 by t-test.

Figure 3. Fasting increases plasma corticosterone and epinephrine levels in L-*G6pc*$^{-/-}$ mice. Hepatocyte-specific *G6pc1* deficiency was induced by tamoxifen injections. Fifteen weeks after tamoxifen injections, (**A**) plasma corticosterone, (**B**) epinephrine and (**C**) norepinephrine levels were measured in the fed condition (ZT1) and again in the same mice after a 6 hour fast (ZT7)

using liquid chromatography tandem mass spectrometry. (n=11-14). Data are shown as mean ± SEM. *p<0.05 by t-test.

Figure 4. Glucocorticoid receptor antagonist mifepristone prevents the fasting-induced decrease in blood Ly6C^{hi} monocytes in L-*G6pc*$^{-/-}$ mice. Hepatocyte-specific *G6pc1* deficiency was induced by tamoxifen injections. Six weeks after tamoxifen injections, mice received an intraperitoneal injection with vehicle or mifepristone (25mg/kg) at the start of the fasting period. (**A**) Total CD45^{+} leukocyte levels were assessed in the fed condition and again in the same mice after a 6 hour fast. Difference in leukocyte levels after the 6 hour fasting period is shown as Δ fasted – fed. (**B**) Quantification of total monocytes, monocyte subsets and neutrophils in the fed and fasted condition, shown as Δ fasted – fed. (n=8-12). Data are shown as mean ± SEM. *p<0.05, **p<0.01, ***p<0.001, by one-way ANOVA.

Figure 5. Fasting increases bleeding time in L-*G6pc*$^{-/-}$ mice. Hepatocyte-specific *G6pc1* deficiency was induced by tamoxifen injections. Over a period of 6-12 weeks after tamoxifen injections, bleeding time was assessed in the fed, fasted, non-fasted and refed condition. (**A**) Bleeding time was recorded during a tail vein bleeding assay. (**B**) Blood volume loss per minute was quantified by measuring absorbance at 550nm using a spectrophotometer. Each data point represents an individual mouse. (n=6-8). Data are shown as mean ± SEM. **p<0.01, ***p<0.001, by t-test. Experiments have been repeated 4 times with similar results.

Figure 6. Effects of hepatocyte-specific *G6pc1* deficiency on plasma levels of coagulation factors. Hepatocyte-specific *G6pc1* deficiency was induced by tamoxifen injections. At 16 weeks after tamoxifen injections (**A**) prothrombin time (PT) and (**B**) activated partial thromboplastin time (APTT) were assessed in the fed and fasted condition. (**C**) Plasma levels of coagulation factor V (FV), (**D**) factor VII (FVII) and (**E**) factor VIII (FVIII) and (**F**) von Willebrand Factor activity (vWF RCF) were measured in the fed and fasted condition. For each experimental condition (fed and 6 hour fast), individual mice were used. (n= 6-8). Data are shown as mean ± SEM. **p<0.01, ***p<0.001, by t-test.

Figure 7. Fasting induces platelet disaggregation in L-*G6pc*$^{-/-}$ mice. Hepatocyte-specific *G6pc1* deficiency was induced by tamoxifen injections. Over a period of 6-16 weeks after tamoxifen injections, blood platelet counts and platelet aggregation were assessed in the fed and fasted condition. (**A**) Blood platelet counts were measured in the fed condition and again in the same mouse after a 6 hour fast. (n=12-16). (**B-C**) Platelet aggregation in response to 10µM ADP in platelet rich plasma was measured using light transmission aggregometry. Representative platelet aggregation responses are shown (**B**) and quantified (**C**). Platelet disaggregation is shown as percentage of maximum aggregation response (**C**). For each experimental condition (fed and 6 hour fast), individual mice were used. (n= 9-11). Data are shown as mean ± SEM. $^{**}p<0.01$, by t-test.

Figure 1

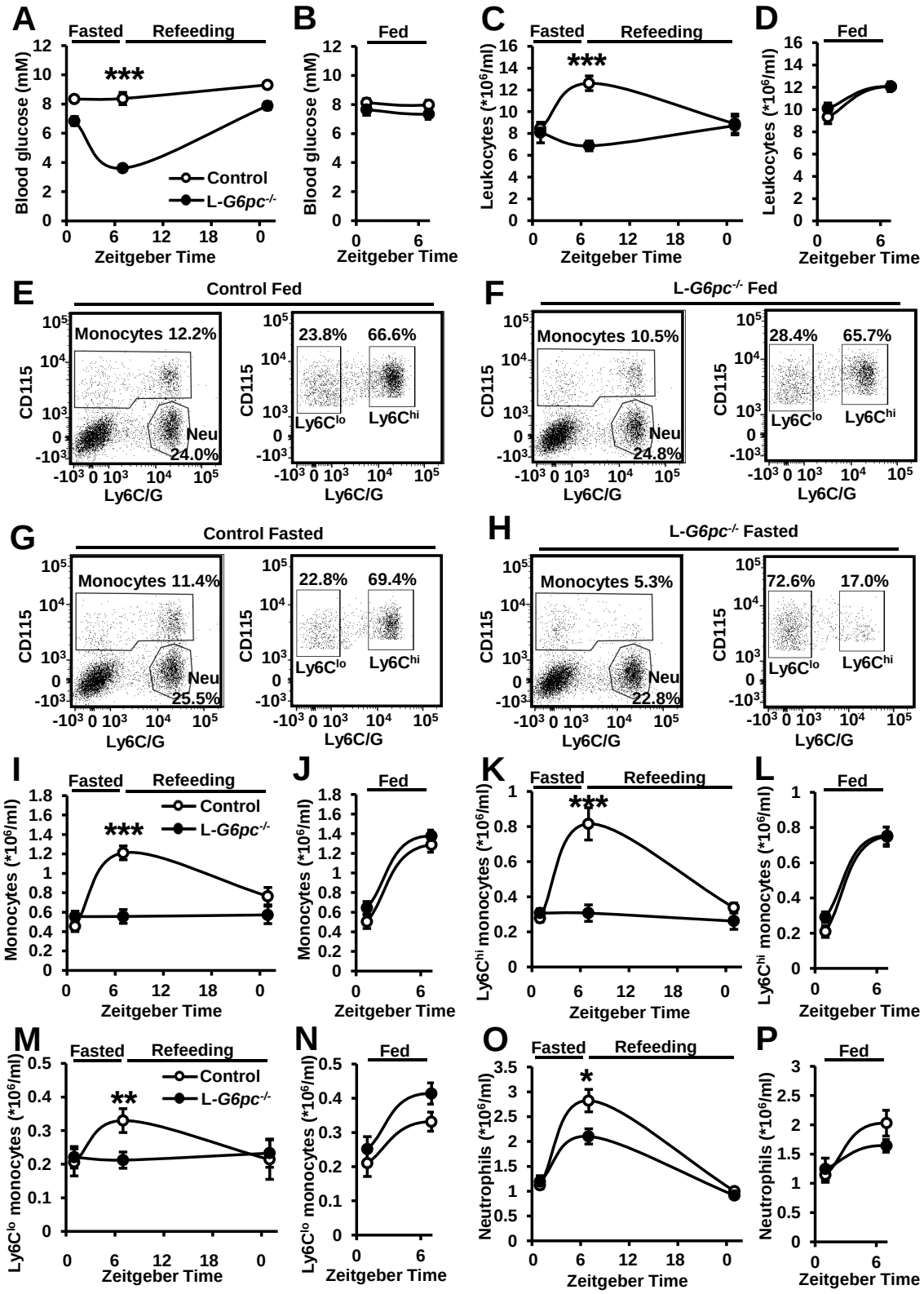
A
Fasted
Refeeding
Blood glucose (mM)
***
Control
L-G6pc-/-
Zeitgeber Time
B
Fed
Blood glucose (mM)
Zeitgeber Time
C
Fasted
Refeeding
Leukocytes (*10^6/ml)
***
Zeitgeber Time
D
Fed
Leukocytes (*10^6/ml)
Zeitgeber Time
E
Control Fed
Monocytes 12.2%
Neu 24.0%
CD115
Ly6C/G
23.8%
66.6%
Ly6Clo
Ly6Chi
F
L-G6pc-/- Fed
Monocytes 10.5%
Neu 24.8%
28.4%
65.7%
G
Control Fasted
Monocytes 11.4%
Neu 25.5%
22.8%
69.4%
H
L-G6pc-/- Fasted
Monocytes 5.3%
Neu 22.8%
72.6%
17.0%
I
Monocytes (*10^6/ml)
J
K
Ly6Chi monocytes (*10^6/ml)
L
M
Ly6Clo monocytes (*10^6/ml)
**
N
O
Neutrophils (*10^6/ml)
*
P

Figure 2

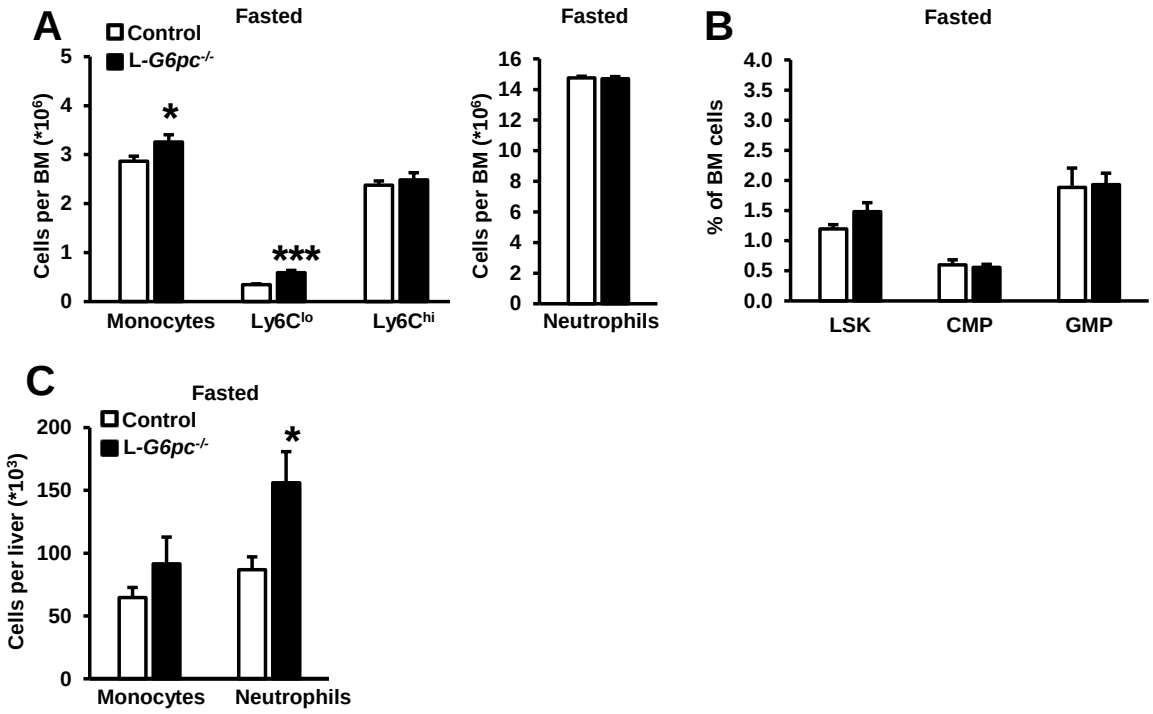
A
Fasted
Control
L-G6pc-/-
Cells per BM (*10^6)
5
4
3
2
1
0
*
***
Monocytes
Ly6Clo
Ly6Chi
Fasted
Cells per BM (*10^6)
16
14
12
10
8
6
4
2
0
Neutrophils
B
Fasted
% of BM cells
4.0
3.5
3.0
2.5
2.0
1.5
1.0
0.5
0.0
LSK
CMP
GMP
C
Fasted
Control
L-G6pc-/-
Cells per liver (*10^3)
200
150
100
50
0
*
Monocytes
Neutrophils

Figure 3

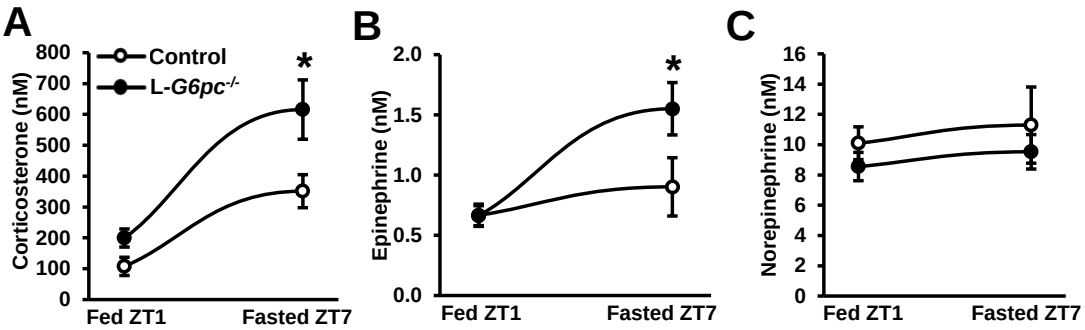
A
Control
L-G6pc-/-
Corticosterone (nM)
800
700
600
500
400
300
200
100
0
*
Fed ZT1
Fasted ZT7
B
Epinephrine (nM)
2.0
1.5
1.0
0.5
0.0
*
Fed ZT1
Fasted ZT7
C
Norepinephrine (nM)
16
14
12
10
8
6
4
2
0
Fed ZT1
Fasted ZT7

Figure 4

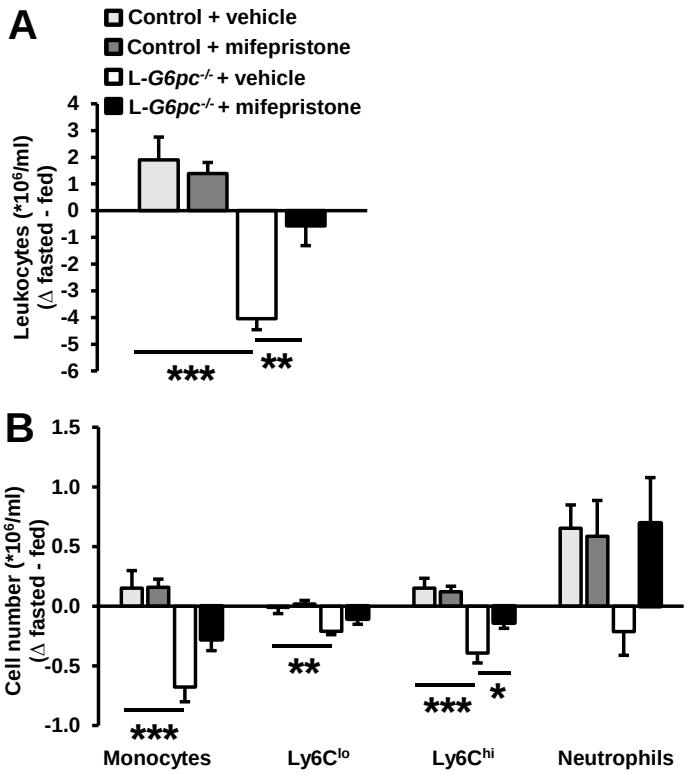
A
Control + vehicle
Control + mifepristone
L-G6pc-/- + vehicle
L-G6pc-/- + mifepristone
Leukocytes (*10^6/ml)
(Δ fasted - fed)
4
3
2
1
0
-1
-2
-3
-4
-5
-6
***
**
B
Cell number (*10^6/ml)
(Δ fasted - fed)
1.5
1.0
0.5
0.0
-0.5
-1.0
***
**
***
*
Monocytes
Ly6C^lo
Ly6C^hi
Neutrophils

Figure 5

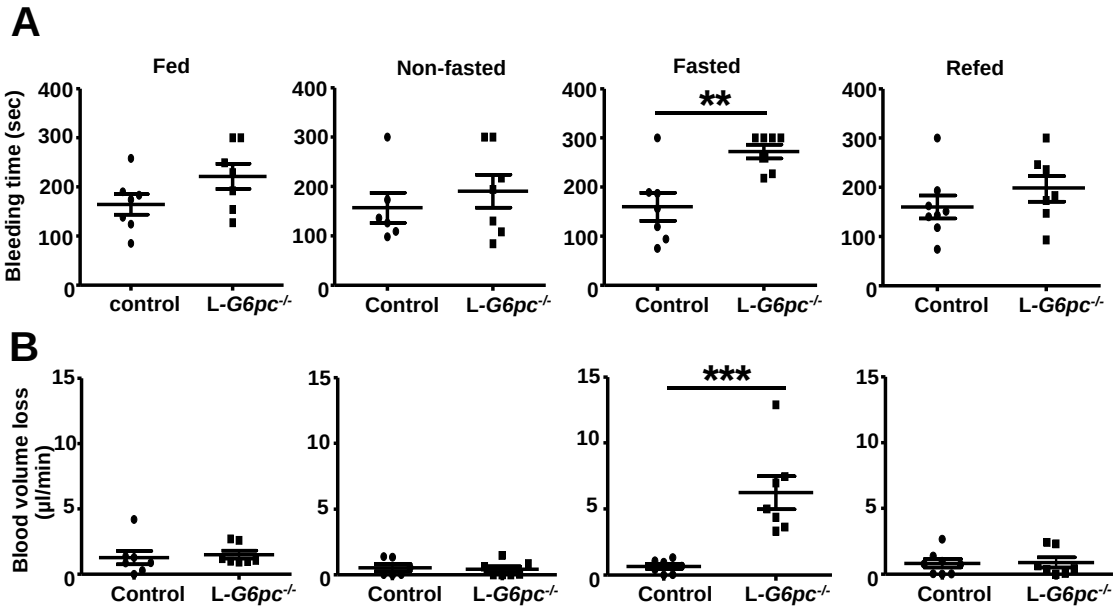
A
Fed
Non-fasted
Fasted
Refed
Bleeding time (sec)
400
300
200
100
0
**
control
Control
L-G6pc-/-
B
Blood volume loss (µl/min)
15
10
5
0
***

Figure 6

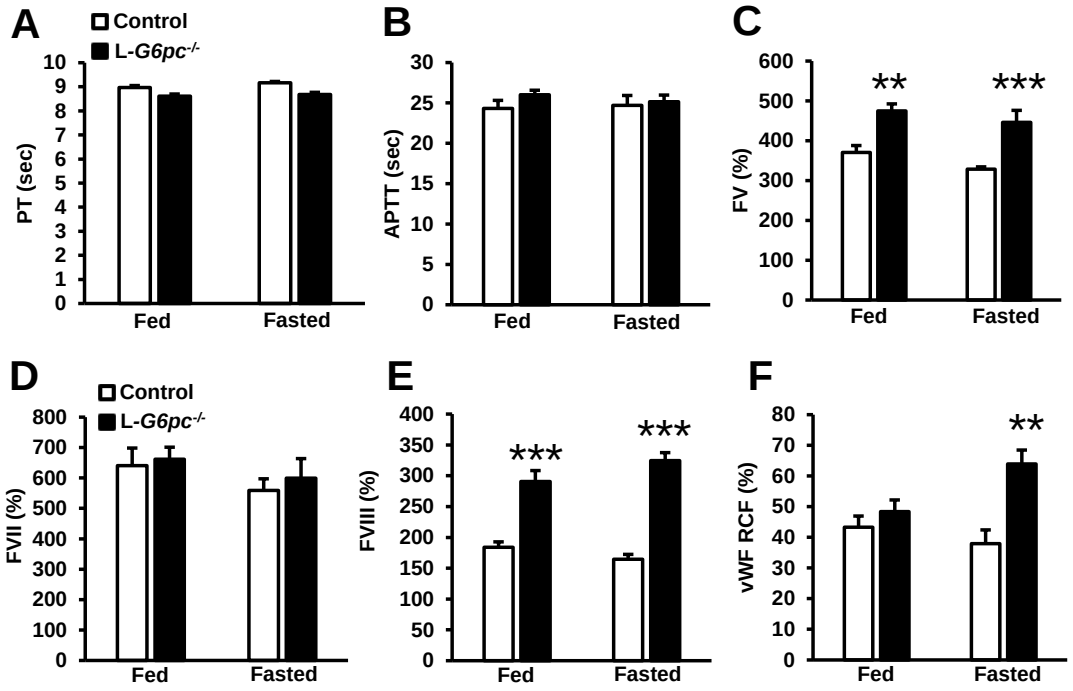
A
Control
L-G6pc-/-
PT (sec)
0
1
2
3
4
5
6
7
8
9
10
Fed
Fasted
B
APTT (sec)
0
5
10
15
20
25
30
Fed
Fasted
C
FV (%)
0
100
200
300
400
500
600
**
***
Fed
Fasted
D
Control
L-G6pc-/-
FVII (%)
0
100
200
300
400
500
600
700
800
Fed
Fasted
E
FVIII (%)
0
50
100
150
200
250
300
350
400
***
***
Fed
Fasted
F
vWF RCF (%)
0
10
20
30
40
50
60
70
80
**
Fed
Fasted

Figure 7

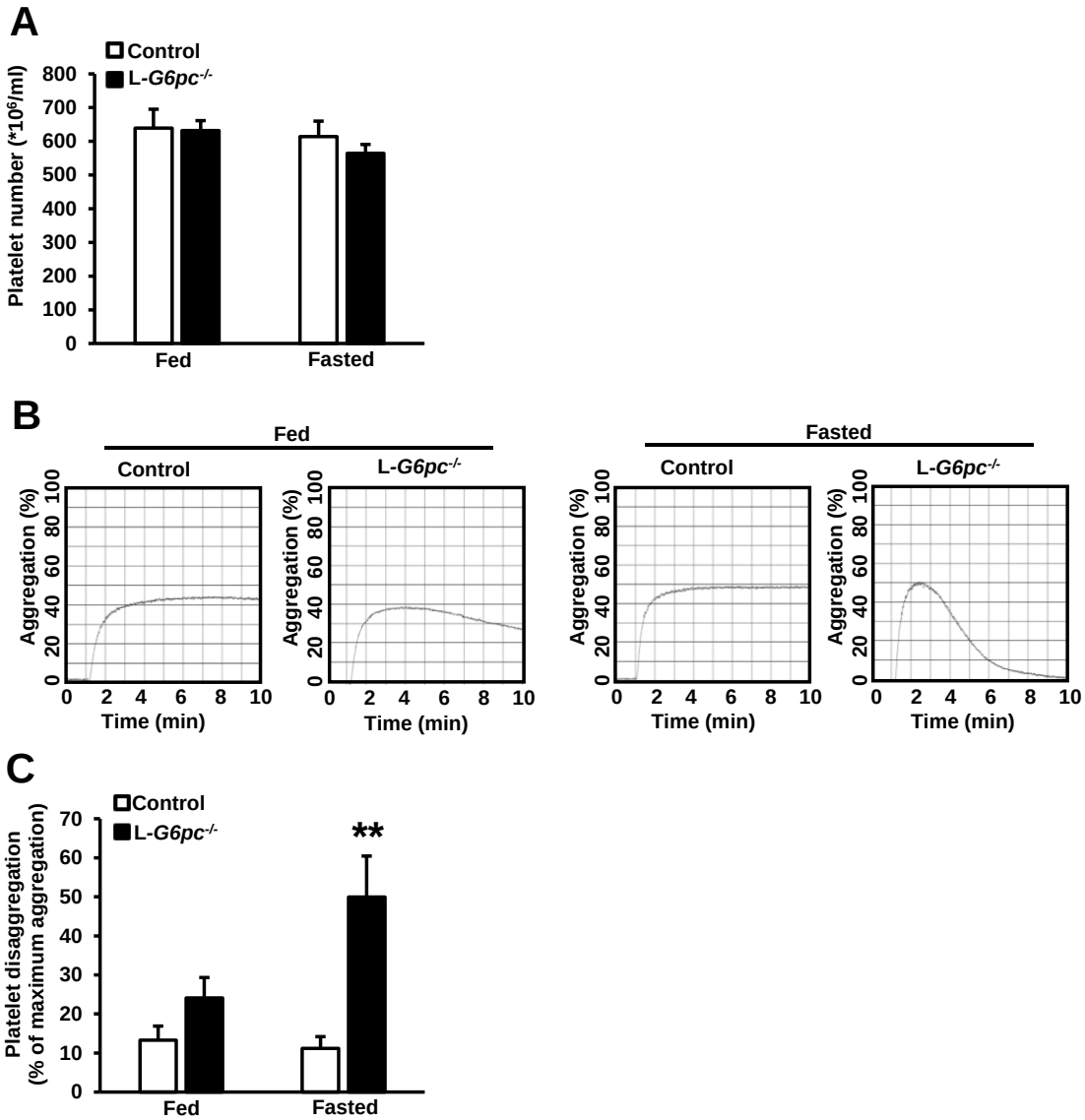
A
Control
L-G6pc-/-
Platelet number (*10^6/ml)
800
700
600
500
400
300
200
100
0
Fed
Fasted
B
Fed
Fasted
Control
L-G6pc-/-
Control
L-G6pc-/-
Aggregation (%)
0 20 40 60 80 100
0 2 4 6 8 10
Time (min)
C
Control
L-G6pc-/-
Platelet disaggregation
(% of maximum aggregation)
70
60
50
40
30
20
10
0
**
Fed
Fasted